CrossMark

Superfluid Gap in Neutron Matter from a Microscopic Effective Interaction

Omar Benhar[1] · **Giulia De Rosi**[2]

Abstract Correlated basis function (CBF) perturbation theory and the formalism of cluster expansions have been recently employed to obtain an effective interaction from a nuclear Hamiltonian strongly constrained by phenomenology. We report the results of a study of the superfluid gap in pure neutron matter, associated with the formation of Cooper pairs in the $^1S_0$ channel. The calculations have been carried out using an improved version of the CBF effective interaction, in which three-nucleon forces are taken into account using a microscopic model. Our results show that a non-vanishing superfluid gap develops at densities in the range $2 \times 10^{-4} \lesssim \rho/\rho_0 \lesssim 0.1$, where $\rho_0 = 2.8 \times 10^{14}$ g cm^{-3} is the equilibrium density of isospin-symmetric nuclear matter, corresponding mainly to the neutron-star inner crust.

Keywords Neutron stars · Superfluidity · Nuclear matter · Correlated basis functions · Cluster expansions

1 Introduction

In neutron stars, both conditions for the occurrence of superfluidity in fermionic systems, that is, strong degeneracy and the existence of an attractive interaction between the constituents of strongly interacting matter, are believed to be fulfilled [1].

The onset of a superfluid (and/or superconducting) phase does not have a significant impact on the equation of state, determining the equilibrium properties of the star, except in the very low-density region of the crust. The condensation energy—i.e. the

✉ Omar Benhar
omar.benhar@roma1.infn.it

1 INFN and Dipartimento di Fisica, Università "La Sapienza", Roma, Rome, Italy

2 INO-CNR BEC Center and Dipartimento di Fisica, Università di Trento, Trento, Italy

difference between the energies of the normal and superfluid states associated with the formation of Cooper pairs [2]—is in fact small, although not totally negligible, with respect to the typical energies of the normal phase [3].

The main effect of the superfluid transition is the opening of an energy gap at the Fermi surface [4]. This leads to a reduction of the phase space available to particles undergoing scattering processes, which in turn results in a strong modification of the neutrino emission, scattering and absorption rates, as well as of the transport coefficients, including the shear viscosity and thermal conductivity. As a consequence, a quantitative understanding of the superfluid phase transition is required to study both neutron-star cooling [5] and the onset of the Chandrasekhar–Friedman–Schutz (CFS) instability of rotating stars [6,7], which is largely driven by dissipative processes [8,9].

The approach based on effective interactions has long been recognized as well suited for the development of a unified description of equilibrium and non-equilibrium properties of nuclear matter, based on realistic models of nuclear dynamics at microscopic level [3,10,11].

In recent implementations, the effective interaction has been derived from realistic phenomenological Hamiltonian—strongly constrained by the available data—within the formalism of correlated basis functions (CBF) [12–16]. Unlike the bare nucleon–nucleon force, the effective interaction is well behaved at short distances and can be used to carry out perturbative calculations in the basis of eigenstates of the non-interacting system.

Existing applications of the CBF effective interaction include calculations of the shear viscosity and thermal conductivity coefficients of neutron matter [13,17], as well as the nuclear matter response to neutrino interactions [12,15,16,18,19]. The potential of the approach based on effective interactions obtained from correlated functions has been recently confirmed by the results of systematic studies of the properties of the Fermi hard-sphere system [20,21], providing a valuable model of nuclear matter.

In this work, we report the results of a calculation of the superfluid gap associated with the formation of Cooper pairs in the $^1S_0$ channel in pure neutron matter (PNM), performed using the CBF effective interaction derived in Refs. [14,15].

The paper is organized as follows. In Sect. 2, we outline the ab initio approach based on a microscopic nuclear Hamiltonian and discuss the derivation of an effective nucleon–nucleon (NN) interaction—suitable to carry out perturbative calculation using the basis states of the non-interacting system—performed combining the CBF formalism and the cluster expansion technique. The differences between the effective interaction and the bare NN potential are also illustrated. The numerical results, indicating the occurrence of a superfluid phase of PNM at densities corresponding to the inner crust of neutron stars, are reported in Sect. 3. Finally, in Sect. 4 we summarize our findings and draw the perspectives for future application of the CBF effective interaction approach.

2 Formalism

In this section, we briefly outline the phenomenological model of nuclear dynamics employed in our work and describe the procedure leading to the determination of the effective interaction.

2.1 The Nuclear Hamiltonian

The formalism of nuclear many-body theory provides a consistent framework, suitable for treating the non-perturbative nature of NN interactions. Within this approach, nuclear matter is modelled as a collection of point-like particles, the dynamics of which are dictated by the Hamiltonian

$$H = \sum_i \frac{\mathbf{p}_i^2}{2m} + \sum_{j>i} v_{ij} + \cdots, \tag{1}$$

where $\mathbf{p}_i$ and m denote the momentum of the ith nucleon and its mass, respectively, v_{ij} is the NN interaction potential and the ellipses refer to the presence of *irreducible* interactions involving three or more nucleons. The inclusion of a three-nucleon potential, V_{ijk}, is in fact necessary to explain the properties of the three-nucleon systems, as well as saturation of isospin-symmetric nuclear matter (SNM).

The NN potential v_{ij} reduces to the Yukawa one-pion exchange potential at large distances, while its behaviour at short and intermediate range is determined by a fit of deuteron properties and NN scattering phase shifts.

Coordinate-space NN potentials are usually written in the form

$$v_{ij} = \sum_p v^p(r_{ij}) O_{ij}^p, \tag{2}$$

where $r_{ij} = |\mathbf{r}_i - \mathbf{r}_j|$ is the distance between the interacting particles, and the sum includes up to eighteen terms. The most prominent contributions are those associated with the operators

$$O_{ij}^{p\leq 6} = [1, (\boldsymbol{\sigma}_i \cdot \boldsymbol{\sigma}_j), S_{ij}] \otimes [1, (\boldsymbol{\tau}_i \cdot \boldsymbol{\tau}_j)], \tag{3}$$

where $\boldsymbol{\sigma}_i$ and $\boldsymbol{\tau}_i$ are Pauli matrices acting in spin and isospin space, respectively, while the operator

$$S_{ij} = \frac{3}{r_{ij}^2} (\boldsymbol{\sigma}_i \cdot \mathbf{r}_{ij})(\boldsymbol{\sigma}_j \cdot \mathbf{r}_{ij}) - (\boldsymbol{\sigma}_i \cdot \boldsymbol{\sigma}_j), \tag{4}$$

reminiscent of the potential describing the interaction between two magnetic dipoles, accounts for the occurrence of non-spherically symmetric forces.

The potential models obtained including the six operators of Eqs. (3)–(4) explain deuteron properties and the S-wave scattering phase shifts up to pion production threshold.

2.2 The CBF Effective Interaction

Performing perturbative calculations in the basis of eigenstates of the non-interacting system requires the replacement of the *bare* NN potential—featuring a strongly repulsive core—with a well-behaved effective interaction [22,23] that can be obtained either summing up ladder diagrams at all orders, as in G-matrix perturbation theory [11,17,24], or modifying the basis states, as in the CBF approach [12,13,17].

Within the CBF formalism, non-perturbative effects are taken into account replacing the states of the non-interacting system, i.e. the Fermi gas states $|n_{FG}\rangle$ in the case of uniform nuclear matter, with a set of *correlated* states, defined as (see, for example, Refs. [25–27])

$$|n\rangle = \frac{F|n_{FG}\rangle}{\langle n_{FG}|F^\dagger F|n_{FG}\rangle^{1/2}}. \tag{5}$$

The operator F, embodying the correlation structure induced by the NN interaction, is written in the form

$$F = \mathcal{S}\prod_{j>i} f_{ij}, \tag{6}$$

with

$$f_{ij} = \sum_p f^p(r_{ij})O_{ij}^p, \tag{7}$$

the two-body operators O_{ij}^p being the same as in Eq. (2). Note that, because the operator structure of f_{ij} reflects the complexity of the NN potential, the product appearing in Eq. (6) needs to be symmetrized through the action of the operator $\mathcal{S}$, to account for the fact that $[f_{ij}, f_{ik}] \neq 0$.

In principle, the radial dependence of the correlation functions $f^p(r_{ij})$ can be determined from functional minimization of the expectation value of the Hamiltonian in the correlated ground state

$$E_V = \langle 0|H|0\rangle. \tag{8}$$

In practice, however, the calculation of the variational energy of Eq. (8) involves non-trivial difficulties. It can be effectively carried out expanding the right-hand side in a series, whose terms describe the contributions of subsystems, or clusters, involving an increasing number of correlated particles (see, for example, Refs. [27,28]). The terms of the cluster expansion can be represented by diagrams, that are classified according to their topological structures. Selected classes of diagrams can then be summed up to all orders solving a set of coupled nonlinear integral equations—referred to as Fermi Hyper-Netted Chain/Single-Operator Chain (FHNC/SOC) equations [26,29]—to obtain an accurate estimate of the ground-state energy. The full derivation of the Euler equation obtained from

$$\frac{\delta E_V}{\delta F} = 0, \tag{9}$$

within the FHNC scheme is discussed in Ref. [30].

The new basis defined by Eq. (5) can be employed to perform perturbative calculations with the *bare* NN potential, although the non-orthogonality of the basis states entails severe computational difficulties [31]. However, the same formalism can be also exploited to obtain an *effective interaction*, suitable to be used with the Fermi gas basis [12,13].

The CBF effective interaction, v^{eff}, is defined through the relation [32]

$$\langle 0|H|0\rangle = \langle 0_{\text{FG}}| \sum_i \frac{\mathbf{p}_i^2}{2m} + \sum_{j>i} v_{ij}^{\text{eff}} |0_{\text{FG}}\rangle, \tag{10}$$

where $|0_{\text{FG}}\rangle$ and $|0\rangle$ denote the Fermi gas and CBF ground state, respectively, and H is the nuclear Hamiltonian of Eq. (1).

In the pioneering works of Refs. [12,13], the left-hand side of Eq. (10) has been evaluated using a truncated version of the state-of-the-art Argonne v_{18} potential, including contributions with $p \leq 6$ [see Eqs. (2)–(4)][33,34] and including two-nucleon cluster contributions only. This approximation leads to the simple expression

$$v_{ij}^{\text{eff}} = \frac{1}{m} \left(\nabla f_{ij}\right)^2 + f_{ij} v_{ij} f_{ij}, \tag{11}$$

where v_{ij} is the bare NN potential and the f_{ij} are determined solving the Euler equations derived from the approximated energy functional, with the correlation range fixed in such a way as to reproduce the FHNC/SOC results obtained with the same Hamiltonian. In Ref. [13], the effects of three- and many-nucleon interactions have been also taken into account, using a density-dependent modification of the NN potential originally proposed in Ref. [35].

More recently, an improved CBF effective interaction has been derived by the authors of Refs. [14–16], who explicitly included three-body cluster contributions to the left-hand side of Eq. (10). This scheme allows for a more realistic treatment of three-body forces, which are known to play a critical role in determining both the spectra of few-nucleon systems and the saturation properties of SNM, based on a realistic description at microscopic level.

The CBF effective interaction of Refs. [14,15] has been obtained from a nuclear Hamiltonian comprising the Argonne v_6' NN potential [34,36] and the Urbana IX (UIX) three-nucleon potential [37]. The v_6' potential accounts for deuteron properties and S-wave NN scattering phase shifts, while the UIX potential, including a Fujita–Miyazawa two-pion exchange attractive term [38] and a purely phenomenological repulsive term, is designed to reproduce the properties of the three-nucleon bound states and the saturation density of SNM.

The energy per particle of both isospin-symmetric nuclear SNM and PNM obtained from v^{eff} in the Hartree–Fock approximation—which reproduces by construction the FHNC/SOC variational results computed using the v_6'+UIX Hamiltonian—turns out
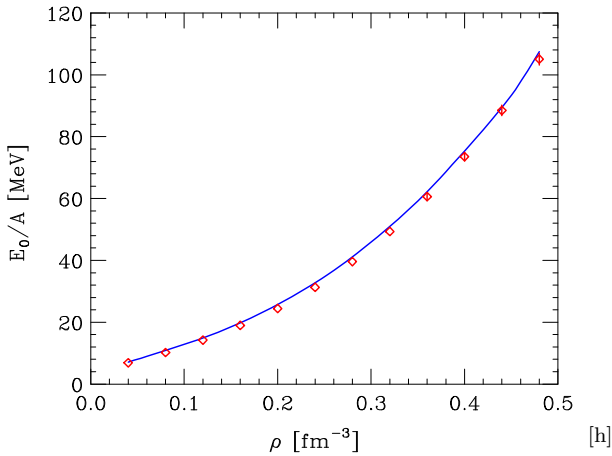
Fig. 1 Energy per particle of PNM as a function of the density, ρ. The solid line represents the energies obtained using the CBF effective interaction—which coincide with the FHNC/SOC energies by construction—while the circles correspond to the values calculated using the Auxiliary Field Diffusion Monte Carlo (AFDMC) technique [39]. Note that the statistical error bars associated with the Monte Carlo energies are only visible $\rho \gtrsim 0.4\ \mathrm{fm}^{-3}$ (Color figure online)
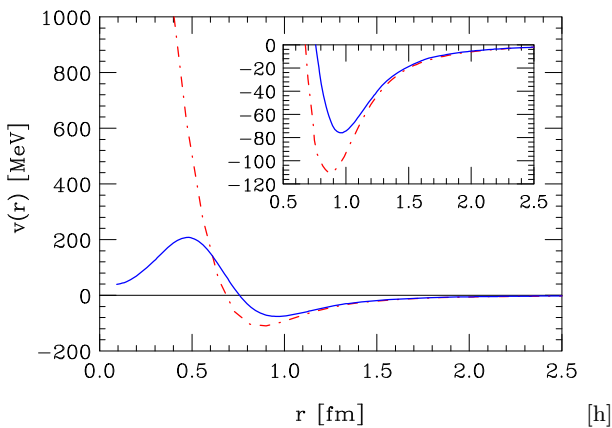
Fig. 2 Nucleon–nucleon potential in the $S = 0$, $T = 1$ channel. The solid and dot–dash lines correspond to the CBF effective interaction of Ref. [15] and to the bare Argonne v_6' [34] potential, respectively. The inset shows a blow-up of the region $0.5 \leq r \leq 2.5$ fm (Color figure online)

to also be in excellent agreement with the results of other highly advanced many-body approaches [15]. Figure 1, showing a comparison with the PNM energies obtained using the Auxiliary Field Diffusion Monte Carlo technique [39], strongly suggests that the FHNC/SOC scheme provides a very accurate upper bound to the ground-state energy.

The solid line of Fig. 2 shows the radial dependence of the CBF effective interaction in the $S = 0$, $T = 1$ channel, S and T being the total spin and isospin of the interacting pair, respectively. Comparison with the dot–dash line, corresponding to the bare v_6'

potential, clearly illustrates the screening effect arising from NN correlations, leading
to the near-disappearance of the short-range repulsive core of the bare interaction. In
addition, due to the modification of the two-nucleon wave function arising from the
inclusion of correlations, the effective interaction includes an additional purely kinetic
term. The inset shows a blow-up of the attractive region.

3 Results

The generalization of the formalism originally derived by Bardeen, Cooper and Schri-
effer [40] to allow the use of correlated basis functions is thoroughly discussed in
Ref. [41]. For any baryon density $\rho = k_F^3/(3\pi^2)$, where k_F denotes the Fermi momen-
tum, the gap equation corresponding to S-wave coupling in cold PNM,

$$\Delta(k) = -\frac{1}{\pi} \int k'^2 dk' \frac{v(k, k')\Delta(k')}{\left[\xi^2(k') + \Delta^2(k')\right]^{1/2}}, \tag{12}$$

has been solved using the algorithm discussed in Ref. [42]. Equation (12) involves in
the momentum-space matrix elements of the potential

$$v(k, k') = \int r^2 dr \, j_0(kr) v^{\text{eff}}(r) j_0(k'r), \tag{13}$$

where $j_0(x) = \sin(x)/x$ is the zeroth-order spherical Bessel function, $v^{\text{eff}}(r)$ is the
projection of the CBF effective potential in the $S = 0$, $T = 1$ channel (see Fig. 2),
and

$$\xi(k) = e(k) - \mu, \tag{14}$$

where $e(k)$ and $\mu = e(k_F)$ denote the energy of a particle carrying momentum k and
the chemical potential, respectively.

The calculation has been carried out using the CBF effective interaction of Refs. [14,
15]. The single-particle spectrum $e(k)$ has been consistently computed at first order
in the CBF effective interaction, that is, within the Hartree–Fock approximation. The
solid line of Fig. 3 illustrates the momentum dependence of the Hartree–Fock spectrum
of PNM at density $\rho = 0.04$ fm^{-1}. For comparison, the kinetic energy spectrum is
also shown, by the dashed line.

The main results of our work are summarized in Fig. 4, showing the superfluid gap
at the Fermi surface, $\Delta(k_F)$, as a function of the Fermi momentum k_F. The solid line
has been obtained using the CBF effective interaction and the Hartree–Fock spectrum,
while the dashed line corresponds to a calculation carried out with the bare v_6' NN
potential and the kinetic energy spectrum. The comparison shows that, while the range
of Fermi momentum in which $\Delta(k_F) \neq 0$ is about the same, the inclusion of interaction
and correlation effects leads to a significant reduction of the gap.

To clarify the roles played by the interaction employed to evaluate the matrix ele-
ment entering Eq. (12) and of the single-particle energies appearing in (14), the results
obtained combining the CBF effective interaction with the kinetic energy spectrum
are also displayed, by the dot–dash line. It appears that while being sizable, the effect
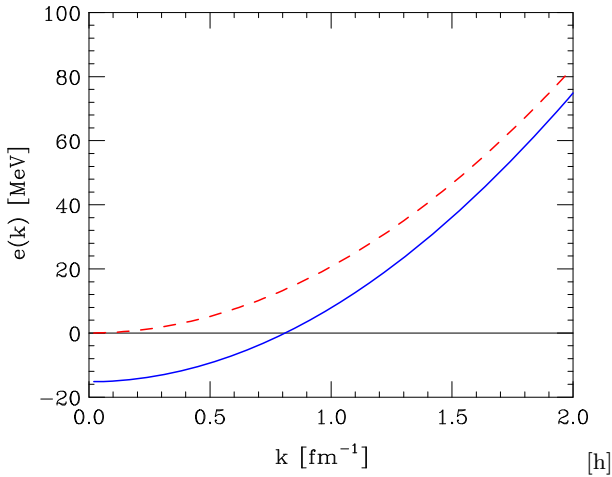
Fig. 3 Momentum dependence of the single-particle spectrum in PNM. Solid line: results obtained at first order in the CBF effective interaction, corresponding to the Hartree–Fock approximation, at $\rho = 0.04\,\mathrm{fm}^{-1}$. Dashed line: kinetic energy spectrum (Color figure online)
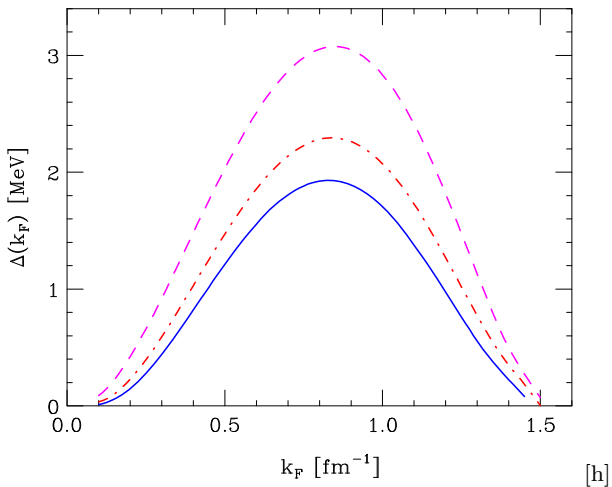
Fig. 4 Fermi momentum dependence of the superfluid gap at the Fermi surface, $\Delta(k_F)$. The dashed line represents the results obtained using the bare v'_6 potential and the kinetic energy spectrum, while the solid line corresponds to calculations carried out using the CBF effective interaction and the Hartree–Fock spectrum. For comparison, the dash-dot line shows $\Delta(k_F)$ computed combining the CBF effective interaction with the kinetic energy spectrum (Color figure online)

of interactions in the single-particle spectrum is not as large as that arising from the replacement of the bare potential with the CBF effective interaction in Eq. (13). In this context, it has to be also kept in mind that second-order contributions, leading to the appearance of an explicit energy dependence of the neutron self-energy, are known to significantly affect $e(k)$ and the nucleon effective mass in the vicinity of the Fermi surface. The impact of these corrections on the determination of $\Delta(k)$ within the proposed approach should be carefully investigated.
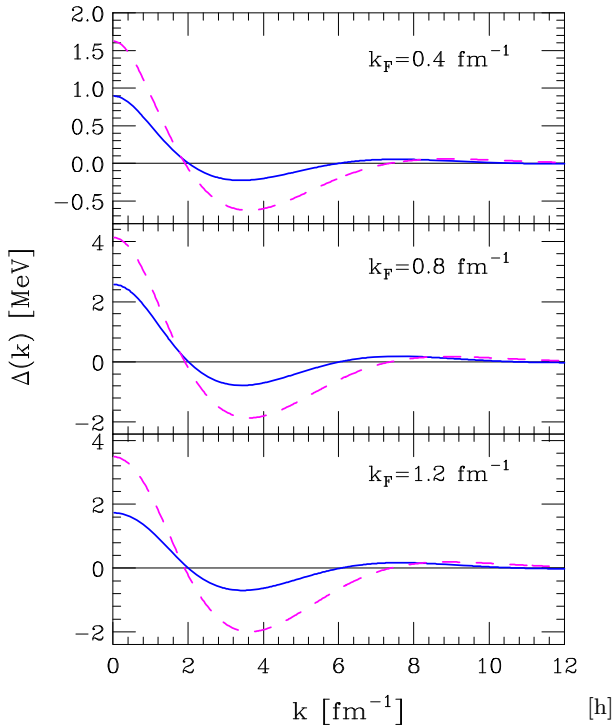
Fig. 5 Momentum dependence of the superfluid gap of Eq. (12). The dashed line shows the results obtained using the bare v_6' potential and the kinetic energy spectrum, while the solid line corresponds to calculations carried out using the CBF effective interaction (Color figure online)

The solid lines of Fig. 5 illustrate the momentum dependence of the gap function, $\Delta(k)$, obtained using the CBF effective interaction for three different values of the Fermi momentum: $k_F = 0.4, 0.8$ and 1.2 fm^{-1}. For comparison, the corresponding results obtained using the bare NN potential and the kinetic energy spectrum are also shown, by the dashed lines.

As a final remark, we note that the present version of the code employed to obtain the numerical results shown in Fig. 4 does not allow to pin down the contribution arising from three-nucleon interactions, unless three-nucleon cluster terms are disregarded altogether. However, in the low-density region in which the superfluid gap is nonzero, two-nucleon interactions are expected to largely dominate.

4 Summary and Outlook

We have carried out a calculation of the superfluid gap in PNM, associated with the formation of Cooper pairs of neutrons in states of total spin $S = 0$ and relative angular momentum $\ell = 0$. The interaction in this channel, which dominates the attractive component of the neutron–neutron force, has been described within the CBF formal-

ism, using an effective potential derived from the state-of-the-art phenomenological models of the two- and three-nucleon potentials referred to as Argonne v_6' and UIX.

Note that the CBF effective interaction is *not* defined in operator form, but only in terms of its expectation value in the Fermi gas ground state. However, unlike the Skyrme-like interactions derived using a similar procedure [45,46], it is strongly constrained by a microscopic model of nuclear dynamics. Therefore, it is well suited to perform calculations of many different quantities, including the nucleon–nucleon scattering rates in matter, needed for a *consistent* description of equilibrium and non-equilibrium properties of neutron stars.

It is important to keep in mind that the validity of the assumption that perturbative calculations involving matrix elements of v_{ij}^{eff} between Fermi gas states provide accurate estimates of quantities other than the ground-state energy cannot be taken for granted, and must be ultimately assessed at numerical level. A step along this line is the work of Refs. [45,46], whose authors employed a CBF effective interaction to carry out calculations of a variety of properties of the Fermi hard-sphere system, ranging from the self-energy to the in-medium scattering cross section and the transport coefficients. The agreement between the results of this study and the predictions of low-density expansions appears to be quite encouraging.

We find that a non-vanishing superfluid gap develops in the density range typical of the neutron-star inner crust, extending from the the neutron drip density $\rho_{ND} \approx 4 \times 10^{11}$ g cm^{-3} to $\rho \approx 10^{14}$ g cm^{-3} [47].

In the case of $^1S_0$ pairing, the critical temperature T_c of the superfluid transition can be estimated from the value of the gap at zero temperature ($T = 0$) [43,44]. The resulting maximum value is in the range $T_c \sim 1 - 2$ MeV, corresponding to $\sim 1 - 2 \times 10^{10}$ K.

Our results, while being interesting in their own right, should be regarded as a first step towards a comprehensive description of the superfluid and superconductive phases of neutron stars. The interaction between neutrons coupled to total spin $S = 1$ and angular momentum $\ell = 1$ is also attractive. The formation of Cooper pairs of neutrons with these quantum numbers is expected to occur at densities $\rho > \rho_0$ typical of the neutron-star core. The appearance of a superfluid phase in this region would strongly affect the dissipative processes determining the stability of rotating stars. In addition, the small fraction—typically less that $\sim 10\%$—of protons are also expected to become superconductive, thus affecting the dissipative processes driven by electromagnetic interactions with electrons and muons. The extension of the formalism employed in our work to study neutron superfluidity in the $^3P_2$ channel and proton superconductivity does not involve any conceptual difficulties.

References

1. M.G. Alford, J.W. Clark, A. Sedrakian, *Pairing in Fermionic Systems: Basic Concepts and Modern Applications* (World Scientific, Singapore, 2006)
2. L.N. Cooper, Bound electron pairs in a degenerate Fermi gas. Phys. Rev. **104**, 1189 (1956)

3. C.-H. Yang, J.W. Clark, Superfluid condensation energy of neutron matter. Nucl. Phys. A **174**, 49 (1971)
4. N.H. March, W.H. Young, S. Sampanthar, *The Many-Body Problem in Quantum Mechanics* (Dover Publications, New York, 1967)
5. D.G. Yakovlev, C.J. Pethick, Neutron star cooling. Annu. Rev. Astron. Astrophys. **42**, 169 (2004)
6. S. Chandrasekhar, Solutions of two problems in the theory of gravitational radiation. Phys. Rev. Lett. **24**, 611 (1970)
7. J.L. Friedman, B.F. Schutz, Lagrangian perturbation theory of nonrelativistic fluids. Astrophys. J. **221**, 937 (1978)
8. N. Andersson, K.D. Kokkotas, The r-mode instability in rotating neutron stars. Int. J. Mod. Phys. D **10**, 381 (2001)
9. N. Andersson, G.L. Comer, K. Glampedakis, How viscous is a superfluid neutron star core? Nucl. Phys. A **763**, 212 (2005)
10. L. Amundsen, E. Østgaard, Superfluidity of neutron matter: (I). Singlet pairing. Nucl. Phys. A **437**, 487 (1985)
11. J. Wambach, T.L. Ainsworth, D. Pines, Quasiparticle interactions in neutron matter for applications in neutron stars. Nucl. Phys. A **555**, 128 (1993)
12. S. Cowell, V.R. Pandharipande, Weak interactions in hot nucleon matter. Phys. Rev. C **73**, 025801 (2006)
13. O. Benhar, M. Valli, Shear viscosity of neutron matter from realistic nucleon–nucleon interactions. Phys. Rev. Lett. **99**, 232501 (2007)
14. A. Lovato, O. Benhar, S. Fantoni, AYu. Illarionov, K.E. Schmidt, Density-dependent nucleon–nucleon interaction from three-nucleon forces. Phys. Rev. C **83**, 054003 (2011)
15. A. Lovato, C. Losa, O. Benhar, Weak response of cold symmetric nuclear matter at three-body cluster level. Nucl. Phys. A **901**, 22 (2013)
16. A. Lovato, O. Benhar, S. Gandolfi, C. Losa, Neutral–current interactions of low-energy neutrinos in dense neutron matter. Phys. Rev. C **89**, 025804 (2014)
17. O. Benhar, A. Polls, M. Valli, I. Vidaña, Microscopic calculations of transport properties of neutron matter. Phys. Rev. C **81**, 024305 (2010)
18. O. Benhar, N. Farina, Correlation effects on the weak response of nuclear matter. Phys. Lett. B **680**, 305 (2009)
19. O. Benhar, A. Cipollone, A. Loreti, Weak response of neutron matter at low momentum transfer. Phys. Rev. C **87**, 014601 (2013)
20. A. Mecca, A. Lovato, O. Benhar, A. Polls, Effective-interaction approach to the Fermi hard-sphere system. Phys. Rev. C **91**, 034325 (2015)
21. A. Mecca, A. Lovato, O. Benhar, A. Polls, Transport properties of the Fermi hard-sphere system. Phys. Rev. C **93**, 035802 (2016)
22. P. Ring, P. Schuck, *The Nuclear Many-Body Problem* (Springer, Berlin, 1980)
23. A.L. Fetter, J.D. Walecka, *Quantum Theory of Many-Particle Systems* (Dover Publications, New York, 2012)
24. H.F. Zhang, U. Lombardo, W. Zuo, Transport parameters in neutron stars from in-medium NN cross sections. Phys. Rev. C **82**, 015805 (2010)
25. E. Feenberg, *Theory of Quantum Fluids* (Academic Press, New York, 1969)
26. V.R. Pandharipande, R.B. Wiringa, Variations on a theme of nuclear matter. Rev. Mod. Phys. **51**, 821 (1979)
27. J.W. Clark, Variational theory of nuclear matter. Prog. Part. Nucl. Phys. **2**, 89 (1979)
28. A. Fabrocini, S. Fantoni, in *First International Course of Condensed Matter Physics*, ed. by D. Prosperi, S. Rosati, G. Violini (World Scientific, Singapore, 1986)
29. S. Fantoni, S. Rosati, Jastrow correlations and an irreducible cluster expansion for infinite boson or fermion systems. Il Nuovo Cimento A **20**, 179 (1974)
30. E. Krotscheck, Fermi-hypernetted chain theory for liquid 3He: a reassessment. J. Low Temp. Phys. **119**, 103 (2000)
31. S. Fantoni, V.R. Pandharipande, Orthogonalization of correlated states. Phys. Rev. C **37**, 1697 (1988)
32. S. Cowell, V.R. Pandharipande, Neutrino mean free paths in cold symmetric nuclear matter. Phys. Rev. C **70**, 035801 (2004)
33. R.B. Wiringa, V.G.J. Stoks, R. Schiavilla, Accurate nucleon–nucleon potential with charge-independence breaking. Phys. Rev. C **51**, 38 (1995)

34. B.S. Pudliner, V.R. Pandharipande, J. Carlson, S.C. Pieper, R.B. Wiringa, Quantum Monte Carlo calculations of nuclei with $A < \sim 7$. Phys. Rev. C **56**, 1720 (1997)
35. I.E. Lagaris, V.R. Pandharipande, Variational calculations of realistic models of nuclear matter. Nucl. Phys. A **359**, 349 (1981)
36. R.B. Wiringa, S.C. Pieper, Evolution of nuclear spectra with nuclear forces. Phys. Rev. Lett. **89**, 182501 (2002)
37. B.S. Pudliner, V.R. Pandharipande, J. Carlson, R.B. Wiringa, Quantum Monte Carlo calculations of $A \leq 6$ nuclei. Phys. Rev. Lett. **74**, 4396 (1995)
38. J.-I. Fujita, H. Miyazawa, Pion theory of three-body forces. Prog. Theor. Phys. **17**, 360 (1957)
39. K.E. Schmidt, S. Fantoni, A quantum Monte Carlo method for nucleon systems. Phys. Lett. B **446**, 99 (1999)
40. J. Bardeen, L.N. Cooper, J.R. Schrieffer, Theory of superconductivity. Phys. Rev. **108**, 1175 (1957)
41. E. Krotscheck, J.W. Clark, Studies in the method of correlated basis functions: (III). Pair condensation in strongly interacting Fermi systems. Nucl. Phys. A **333**, 77 (1980)
42. V.A. Khodel, V.V. Khodel, J.W. Clark, Solution of the gap equation in neutron matter. Nucl. Phys. A **598**, 390 (1996)
43. D.R. Tilley, J. Tilley, *Superfluidity and Superconductivity* (CRC Press, Boca Raton, 1990)
44. J.M.C. Chen, J.W. Clark, R.D. Davé, V.V. Khodel, Pairing gaps in nucleonic superfluids. Nucl. Phys. A **555**, 59 (1993)
45. J. Rikovska Stone, J.C. Miller, R. Koncewicz, P.D. Stevenson, M.R. Strayer, Nuclear matter and neutron-star properties calculated with the Skyrme interaction. Phys. Rev. C **68**, 034324 (2003)
46. E. Chabanat, P. Bonche, P. Haensel, J. Meyer, R. Schaeffer, A Skyrme parametrization from subnuclear to neutron star densities. Nucl. Phys. A **627**, 710 (1997)
47. N. Chamel, P. Haensel, Physics of neutron star crusts. Living Rev. Relativ. **11**, 10 (2008)